Monthly Notices of the ROYAL ASTRONOMICAL SOCIETY

MNRAS **469,** S506–S516 (2017) doi:10.1093/mnras/stx2002
Advance Access publication 2017 August 5

Nitrogen-to-carbon atomic ratio measured by COSIMA in the particles of comet 67P/Churyumov–Gerasimenko

Nicolas Fray,[1⋆] Anaïs Bardyn,[1,2] Hervé Cottin,[1] Donia Baklouti,[3] Christelle Briois,[2] Cécile Engrand,[4] Henning Fischer,[5] Klaus Hornung,[6] Robin Isnard,[1,2] Yves Langevin,[3] Harry Lehto,[7] Léna Le Roy,[8] Eva Maria Mellado,[6] Sihane Merouane,[5] Paola Modica,[1,2] François-Régis Orthous-Daunay,[9] John Paquette,[5] Jouni Rynö,[10] Rita Schulz,[11] Johan Silén,[10] Sandra Siljeström,[12] Oliver Stenzel,[5] Laurent Thirkell,[2] Kurt Varmuza,[13] Boris Zaprudin,[7] Jochen Kissel[5] and Martin Hilchenbach[5]

Affiliations are listed at the end of the paper

Accepted 2017 August 2. Received 2017 August 2; in original form 2017 March 28

ABSTRACT

The COmetary Secondary Ion Mass Analyzer (COSIMA) on board the *Rosetta* mission has analysed numerous cometary dust particles collected at very low velocities (a few m s^{-1}) in the environment of comet 67P/Churyumov–Gerasimenko (hereafter 67P). In these particles, carbon and nitrogen are expected mainly to be part of the organic matter. We have measured the nitrogen-to-carbon (N/C) atomic ratio of 27 cometary particles. It ranges from 0.018 to 0.06 with an averaged value of 0.035 ± 0.011. This is compatible with the measurements of the particles of comet 1P/Halley and is in the lower range of the values measured in comet 81P/Wild 2 particles brought back to Earth by the *Stardust* mission. Moreover, the averaged value found in 67P particles is also similar to the one found in the insoluble organic matter extracted from CM, CI and CR carbonaceous chondrites and to the bulk values measured in most interplanetary dust particles and micrometeorites. The close agreement of the N/C atomic ratio in all these objects indicates that their organic matters share some similarities and could have a similar chemical origin. Furthermore, compared to the abundances of all the detected elements in the particles of 67P and to the elemental solar abundances, the nitrogen is depleted in the particles and the nucleus of 67P as was previously inferred also for comet 1P/Halley. This nitrogen depletion could constrain the formation scenarios of cometary nuclei.

Key words: astrochemistry – space vehicles – comets: general – comets: individual: 67P/Churyumov – Gerasimenko – meteorites, meteors, meteoroids.

1 INTRODUCTION

Comets are thought to be among the least altered objects in the Solar system (Willacy et al. 2015). Therefore, their composition could reflect the processes present in the solar nebula at the time of the planetesimal formation. *In situ* investigations of cometary material providing new constraints on the formation of the comets and of the Solar system itself constitute one of the main scientific goals of the *Rosetta* mission (Glassmeier et al. 2007). The first *in situ* chemical analyses of cometary particles were performed by the PIA and PUMA mass spectrometers on board the *Giotto* and *Vega* missions during the flyby of comet 1P/Halley (Kissel et al. 1986a; Kissel et al. 1986b). These analyses have highlighted large amounts of light elements such as carbon, hydrogen, oxygen and nitrogen, originating probably essentially from organic components embedded in the cometary particles (Clark et al. 1987; Langevin et al. 1987; Lawler & Brownlee 1992; Fomenkova et al. 1994). Due to the very high velocities of the Halley flybys, most of the ions created upon impact were mono-atomic and only a small fraction were polyatomic (Kissel & Krueger 1987). Thus, a more detailed chemical characterization of the organic matter present in cometary particles was challenging. Nevertheless, some tentative identifications of specific organic compounds have been reported (Kissel & Krueger 1987; Fomenkova et al. 1994; Fomenkova 1999). The elemental abundances measured in the particles of comet 1P/Halley

⋆ E-mail: nicolas.fray@lisa.u-pec.fr

at that time were mainly reported by Jessberger et al. (1988; 1991). The carbon abundance, averaged over a large number of mass spectra, is about 10 times higher in the particles of 1P/Halley than in CI carbonaceous chondrites (Jessberger et al. 1988). This indicates that comets are extremely rich in carbonaceous matter. The predominance of organic matter in cometary particles has been confirmed by the *in situ* mass spectrometry analysis performed during the flyby of comet 81P/Wild 2 by the *Stardust* spacecraft (Kissel et al. 2004).

The *Stardust* spacecraft has returned to Earth samples of cometary particles collected in the coma of comet 81P/Wild 2 (Brownlee et al. 2006). The laboratory analyses of these particles demonstrated the presence of minerals formed at high temperature (Brownlee et al. 2006; Brownlee 2014). Organic matter has also been detected for which some chemical structures have been proposed (Cody et al. 2008), and some molecules, such as methylamine and glycine, have been identified (Elsila et al. 2009). Additionally, atomic ratios, such as O/C and N/C, have been measured (Keller et al. 2006; Sandford et al. 2006; Cody et al. 2008; De Gregorio et al. 2011). However, the measurement of the carbon abundance and the characterization of the organic matter were compromised as the particles were altered by the high-speed collection in aerogel. Moreover, some potential contaminations of the aerogel could have greatly complicated the characterization of the organic matter present in these samples (Sandford et al. 2010). Nevertheless, some of the *Stardust* samples contain relatively unaltered, refractory cometary material, and it has been suggested that the refractory organic matter present in these samples is dominated by an insoluble organic matter (IOM) and highly aromatic organic matter (De Gregorio et al. 2011).

In addition to *in situ* studies and the *Stardust* returned samples, the composition of comets can also be investigated by analysing cosmic dust particles collected in the Earth's stratosphere and in Antarctic snow. Some fraction of these cosmic dust particles are thought to be cometary grains (Dobrica et al. 2009; Brownlee 2016; Flynn et al. 2016; Sandford et al. 2016). In particular, the anhydrous interplanetary dust particles (IDPs), which have a higher carbon content compared to the most carbon-rich meteorites, are widely thought to be samples of comets (Thomas et al. 1993; Keller et al. 2004).

On board the *Rosetta* orbiter, the study of the composition of cometary particles was mainly performed by the COSIMA instrument (see next section, for a brief description of this instrument). It was designed to determine the composition of cometary dust particles by Time-Of-Flight Secondary Ions Mass Spectrometry (TOF-SIMS; Kissel et al. 2007). The solid organic matter detected in cometary dust particles by COSIMA shares some similarities with the IOM extracted from carbonaceous chondrites (Fray et al. 2016). While the elemental abundances of C, O, Na, Mg, Al, Si, K, Ca, Cr, Mn and Fe are reported by Bardyn et al. (2017), a specific focus on the N/C atomic ratio is given in this paper. The N/C atomic ratio in extraterrestrial samples, such as carbonaceous chondrites, micrometeorites and IDPs, is varying over a wide range of values from close to 0 up to 0.2 (Aleon et al. 2003; Matrajt et al. 2003; Alexander et al. 2007; Dartois et al. 2013). In the particles of 81P/Wild 2 brought back to Earth by the *Stardust* mission, the N/C atomic ratio is also spanning over a wide range from 0.002 to 0.18 (De Gregorio et al. 2011). In this study, we report for the first time the N/C atomic ratio of 27 cometary particles collected in the environment of 67P/Churyumov–Gerasimenko (hereafter 67P). We compare these values with those measured in other comets, carbonaceous chondrites, micrometeorites and IDPs. This comparison will highlight the similarities as well as the differences between those extraterrestrial materials and will help to constrain the origin of the cometary organic matter, which contains most of the carbon and nitrogen.

Moreover, it has been shown that the C/Si atomic ratio of the nucleus and of the particles of 1P/Halley is close to the solar value (Geiss 1987; Jessberger et al. 1988). Nevertheless, the N/C and N/Si atomic ratios are about six times lower in 1P/Halley than in the Sun, showing that nitrogen is depleted in 1P/Halley as compared to the Sun (Geiss 1987; Wyckoff et al. 1991). Thus, we will also consider the global nitrogen abundance in 67P to determine if the nitrogen depletion is particular only to 1P/Halley or not.

2 METHODS

2.1 The COSIMA instrument

The COmetary Secondary Ion Mass Analyzer (COSIMA) experiment on the ESA's *Rosetta* mission was designed to capture, image and determine *in situ* the composition of cometary dust particles. A complete description of the COSIMA instrument is available in Kissel et al. (2007). A total of 24 target holders, each with three 10×10 mm^2 collection targets, most of them covered by a thin layer of gold black (Hornung et al. 2014), can be moved in front of a dust funnel so that cometary dust entering the instrument hits the collection target and adheres to it. Depending on the trajectory of the spacecraft around the nucleus of 67P, the collection velocity was between 0.1 and 20 m s^{-1} (Della Corte et al. 2015; Rotundi et al. 2015; Merouane et al. 2016). These values are rather low compared to the 6 km s^{-1} collection velocity of the *Stardust* mission (Brownlee et al. 2006), the impact velocity of 79.2 and 76.8 km s^{-1} for the PUMA-1 and 2 instruments on the *Vega*-1 and 2 spacecraft (Sagdeev et al. 1986), and 68.4 km s^{-1} for the PIA instrument on the *Giotto* spacecraft (Reinhard 1986). Such a low capture velocity in the COSIMA instrument ensured that the composition of the cometary particles was not altered by the collection process. After exposure to the cometary environment, the target holders were first moved in front of an internal microscope, named COSISCOPE, to be imaged with a spatial resolution of 14 μm (Hornung et al. 2016; Langevin et al. 2016) and then moved in front of a beam of positive indium ions $^{115}In^+$ for TOF-SIMS analyses. The primary ion beam was generated by a liquid indium ion source at 8 keV and was pulsed (about 1000 ions per pulse within 3 ns with a 1.5 kHz repetition rate) and focused on the sample to be analysed (Kissel et al. 2007). The footprint of the primary ions beam at the surface of the sample, defined as the full width at half-maximum (FWHM) of the intensity of the peak, is about 35×50 μm^2 (Hilchenbach et al. 2016). These primary $^{115}In^+$ ions impact on the solid sample (i.e. the cometary dust particle) and sputter secondary ions and neutrals from the surface of the sample. The secondary ions are collected and directed into a reflectron time-of-flight (TOF) system. The measured TOFs of the secondary ions are then converted into mass over charge (m/z) ratios. The COSIMA mass spectrum of secondary ions is produced with a mass resolution $m/\Delta m$ of about 1400 at half peak maximum at $m/z = 100$ (Hilchenbach et al. 2016). This resolution enables in most cases the distinction of elemental ions from hydrogen-containing organic ions at a given integer mass for $m/z < 100$. All the mass spectra considered in this paper are the result of 2.5-min acquisitions. It should be noted that in order to save the primary ion source and ensure it to last for the entire 2 yr *Rosetta* mission, no sputtering was performed on samples before the analyses presented in this paper. COSIMA is not equipped with an electron flood gun. Thus, the charge of the cometary particles, resulting from the implantation of primary $^{115}In^+$ ions, cannot be

Table 1. Characteristics of the N/C calibration samples analysed with the COSIMA RM, including target numbers, size, the N/C atomic ratio from the literature, the measured CN^-/C_2^- ion ratio and the analysis date.

	Target	Sample	Classification		Size (μm^2)	N/C (at.)	Reference	CN^-/C_2^-	Date of analysis
1	4B8	Allende	CV 3	Bulk	350 × 420	0.005 ± 0.001	Kerridge (1985)	0.53 ± 0.04	23/03/2013
2	4B7	Lance	CO 3	Bulk	350 × 200	0.007	Kerridge (1985)	0.49 ± 0.04	30/03/2013
3	4B8	Lance	CO 3	Bulk	300 × 380	0.007	Kerridge (1985)	0.61 ± 0.07	29/03/2013
4	4DC	GRO 95 502	OC 3	IOM	600 × 500	0.007	Alexander et al. (2007)	0.24 ± 0.03	15/06/2013
5	4DC	Murchison	CM 2	IOM	370 × 230	0.0327 ± 0.0001	Alexander et al. (2007)	0.58 ± 0.05	14/06/2013
6	4E1	Renazzo	CR 2	Bulk	470 × 450	0.0341	Alexander et al. (2012)	0.87 ± 0.08	24/07/2013
7	4DC	Orgueil	CI 1	IOM	340 × 380	0.0349 ± 0.0001	Alexander et al. (2007)	0.75 ± 0.05	15/06/2013
8	4B7	Murchison	CM 2	Bulk	300 × 200	0.0433	Alexander et al. (2012)	1.14 ± 0.09	30/03/2013
9	4B8	Murchison	CM 2	Bulk	400 × 400	0.0433	Alexander et al. (2012)	0.81 ± 0.07	29/03/2013
10	48A	DC 94	UCAMM	Bulk	65 × 50	0.05 ± 0.01	Dartois et al. (2013)	1.12 ± 0.03	20/12/2011

compensated. During the 2 yr mission, more than 30 000 particles and particle fragments have been collected and imaged, and some of them have been successfully analysed by TOF-SIMS. The particles that were detected on the optical images have sizes ranging from one pixel (about 14 μm) to about 800 μm (Langevin et al. 2016). The large number of collected particles allowed us to determine their cumulative size distribution (Merouane et al. 2016, 2017). The particles can be classified according to their morphology into two main types: the compact particles and the porous clusters. Most of the clusters seem to originate from large aggregates that disrupted shortly before collection. Their morphologies allow further classification into three sub-groups, i.e. shattered clusters, glued clusters and rubble piles (Langevin et al. 2016). Moreover, the detailed inspection of the optical images has revealed that the clusters are made of smaller units of typically several tens of micrometers and have a tensile strength of about 10^3 Pa (Hornung et al. 2016). COSIMA cannot investigate the structure of the samples at a scale smaller than ∼10 μm, but MIDAS (Micro-Imaging Dust Analysis System) images show a substructure of the particles with size units comparable to those observed in IDPs and micrometeorites (Bentley et al. 2016). At the size scale of the primary ion beam of COSIMA (about 35 × 50 μm^2), the cometary particles are always made of a mixture of minerals and organic matter. Indeed, the positive ion mass spectra contain some organic ions (mainly $^{12}C^+$, CH^+, CH_2^+, CH_3^+ and $C_2H_3^+$) and rock-forming elements such as $^{23}Na^+$, $^{24}Mg^+$, $^{28}Si^+$ and $^{56}Fe^+$ (Fray et al. 2016). Results about the composition of dust particles have already been published (Fray et al. 2016; Hilchenbach et al. 2016; Bardyn et al. 2017; Stenzel et al. 2017), but we concentrate here on the measurements of the N/C atomic ratio in 67P dust particles.

2.2 Calibration samples

To retrieve quantitative information from TOF-SIMS analyses, specific calibration experiments have been performed with a ground-based reference instrument (RM) identical to the flight model (XM) of COSIMA (Le Roy et al. 2012; Krueger et al. 2015; Le Roy et al. 2015b). They provided relative sensitivity factors for positive secondary ions for a large set of elements from the analysis of a set of calibration samples (Krueger et al. 2015) and are complemented with further data by Bardyn et al. (2017). Here, we report a calibration for the measurement of the N/C atomic ratio for which we have used the negative secondary ion mass spectra and more specifically the CN^-/C_2^- ion ratio as recommended by Thomen et al. (2014). It has been shown, from dynamic SIMS measurements and from a simple analytical model (Thomen et al. 2014), that the measurement of the N/C atomic ratio on rough organic surfaces is improved by using CN^-/C_2^- instead of CN^-/C^-. Indeed, CN^-/C^- should vary linearly with the nitrogen content of the analysed surface, whereas CN^-/C_2^- should vary linearly with the N/C atomic ratio (Thomen et al. 2014). To calibrate the COSIMA instrument, samples of bulk carbonaceous chondrites, IOM extracted from carbonaceous chondrites and a fragment of one ultra-carbonaceous Antarctic micro-meteorite (UCAMM) were studied (see Table 1). These samples contain carbonaceous matters that should be rather good analogues to the organic matter found in cometary dust particles (Fray et al. 2016). Note that some of these samples are mostly composed of organic matter, such as the IOM samples, whereas others contain a mixture of minerals and organic matter, such as the bulk samples of meteorites. All samples were pressed against a sapphire window into gold targets pre-heated at 900°C for 10 min. Table 1 summarizes the N/C atomic ratios (ranging from 0.5 to 5 per cent) of the studied samples gathered from the literature (Kerridge 1985; Alexander et al. 2007; Alexander et al. 2012; Dartois et al. 2013) as well as the measured CN^-/C_2^- ion ratios.

2.3 Calibration of the N/C atomic ratio

For the calibration samples analysed with the reference model (RM), we have selected between 2 and 12 negative ion mass spectra with the lowest intensities of gold and polydimethylsiloxane (PDMS) fragments. The latter is one of the most common contaminants observed in TOF-SIMS (Vickerman & Briggs 2013; Henkel & Gilmour 2014). This selection method ensures that nearly all the CN^- and C_2^- ions detected in these mass spectra originate from the calibration samples. Even though fragment ions of PDMS (mainly CH_3SiO^- and $CH_3SiO_2^-$) as well as gold ions (Au^-) were still detectable in the mass spectra, their intensities were much lower (at least a factor of 10 and sometimes a factor of 100) than in the spectra on the target. Indeed, the size of the calibration samples (more than 200 μm, see Table 1) is considerably larger than the beam size (about 35 × 50 μm^2 at FWHM). Therefore, the contribution of the contamination in the negative ion mass spectra acquired on the calibration samples is negligible. The total number of counts for the C_2^- peaks was obtained by adding the intensity acquired for all relevant TOF channels over the full width of this peak. The same method has been applied for the CN^- peak. For each value, we have associated a statistical error bar equal to the square root of the total number of counts. Then, the CN^-/C_2^- ion ratio has been calculated as well as its associated relative error bar, which is equal to the sum of the relative error bars of the total number of counts of CN^- and C_2^-. Due to the low intensity of the contamination in the mass spectra, it was not necessary to subtract the possible contribution of

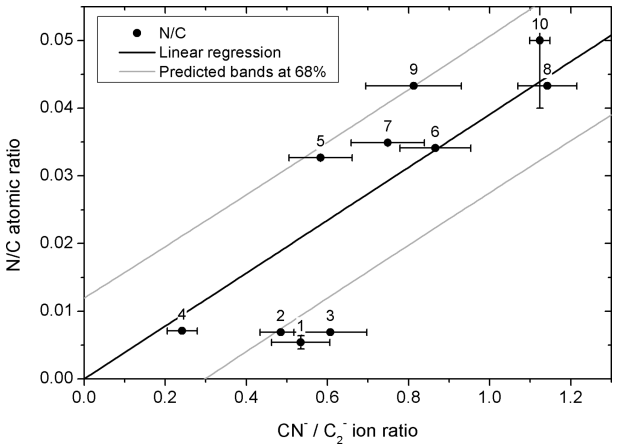

Figure 1. Calibration curve of the N/C atomic ratio as a function of the CN^-/C_2^- ion ratio. The black dots refer to the 10 extraterrestrial calibration samples (see Table 1), with corresponding numbers. The black line is the linear regression passing through the origin and the grey lines are the predicted range with a level of confidence of 68 per cent.

the contamination. The resulting values of the CN^-/C_2^- ion ratios are indicated in Table 1 and in Fig. 1.

Fig. 1 presents the N/C atomic ratio of the 10 calibration samples as a function of the measured CN^-/C_2^- ion ratios. The black line is the best linear fit passing through the origin, and the grey lines are the predicted bands at 68 per cent level of confidence. The slope of the linear regression is 0.04. This is in good agreement with the calibration presented in Le Roy et al. (2015b; with slope 0.036). This previous calibration was based on the study of pure organic molecules with a well-defined structure and an N/C atomic ratio ranging from 0.4 to 1. Thus, even though two calibrations curves were obtained on different samples (pure semi-volatile organic molecules and macromolecular organic matter mixed with minerals), their slopes are in fairly close agreement. The ten measurements used for calibration show a rather large dispersion (see Fig. 1), which cannot be explained only by the error bars on the CN^-/C_2^- ionic ratios. Nevertheless, we have to keep in mind that we have used the bulk N/C elemental ratios of the carbonaceous chondrites and of the IOMs (see Table 1). But these natural samples are heterogeneous and the actual N/C elemental ratio of samples at the location of the COSIMA RM measurements could be slightly different from the bulk samples. This heterogeneity is well illustrated by the two different samples (numbered 8 and 9, see Fig. 1 and Table 1) of the bulk Murchison chondrite, which present very different CN^-/C_2^- ionic ratios. Thus, the dispersion of the calibration measurements is surely mostly due to the heterogeneity of the natural samples that we have used. Consequently, even if the CN^-/C_2^- ion ratio is determined on the cometary particles with a great accuracy, the final error bars of the final N/C atomic ratio will be at least $\pm$ 0.01.

2.4 COSIMA mass spectra of cometary particles

As the size of the primary ion beam is quite large (about 35 $\times$ 50 μm^2 at FWHM), all COSIMA mass spectra acquired on board *Rosetta* contain a contribution originating from the target itself and from the surface contamination. Thus, almost all the negative ion mass spectra contain some Au^- ions (196.97 amu) as well as some fragment ions of PDMS. Two characteristic fragment ions of PDMS in negative mode are CH_3SiO^- (59.00 amu) and $CH_3SiO_2^-$ (74.99 amu). Besides PDMS, other compounds are also present in the surface contamination. Indeed, we can observe elemental ions from elements with a high electronegativity (such as fluorine, chlorine, bromine, and iodine as well as oxygen and sulphur) in the negative ion mass spectra obtained from the collection targets before their exposure to the comet environment. It shows that PDMS is not the only surface contaminant present on the COSIMA targets. Nevertheless, by comparing the spectra obtained on the target and on the cometary particles, it is possible to undoubtedly determine the contribution from the cometary particles. It has already been shown that some C^-, CH^-, O^- and OH^- ions in COSIMA spectra originate from the cometary particles (Fray et al. 2016; Bardyn et al. 2017). Fig. 2 displays negative ion mass spectra at several masses of interest (in a vertical logarithmic scale) acquired on three different cometary particles (in red) and on the same collection target close to the considered particle (in black). To increase the signal-to-noise ratio, the mass spectra displayed in red are the sum of several individual mass spectra acquired at adjacent positions on a particle. Therefore, these spectra represent an average spectrum of the particle and cannot reflect possible compositional heterogeneities of the particle. The mass spectra displayed in black are also the sum of individual spectra acquired on the target normalized to the intensity of the PDMS fragments present in the mass spectra acquired on the particles (CH_3SiO^-: 59.00 amu and $CH_3SiO_2^-$: 74.99 amu). Therefore, Fig. 2 highlights the changes of the ion intensities between the particles and the target locations. For example, the $C^-/CH_3SiO_2^-$ ion ratio increases by a factor of at least 5 between the target and the particle. In Fig. 2, it can be seen that in the spectra of the target, a secondary peak is located on the left-hand side of the main peak (i.e. at 11.95, 23.89 and 25.88 amu for the C^-, C_2^- and CN^- peaks, respectively) with an intensity of about 2 per cent of the main peak. This peak originates from the electrons generated by the collisions between the considered ions and the last grid of the reflectron that is located 2.85 mm in front of the detector. For the mass spectra obtained on the particles, we can also observe for some peaks a long shoulder towards the left-hand side of the main peak. For the C^- peak, this shoulder extends from about 11.85 to 12 amu in the spectra acquired on the selected particles and presented in Fig. 2. This left-hand shoulder is ubiquitous for the negative ion mass spectra performed on the cometary particles. The cometary particles are poor electric conductors and their surface is positively charged by the implantation of the In^+ primary ions (Hilchenbach et al. 2017). As COSIMA is not equipped with an electron flood gun, this charge cannot be compensated. The negative ions ejected from the charged particle's surface experience a reduced extraction voltage and thus reach a lower velocity as compared to those originating from the conducting and uncharged collection target. Contrary to expectations, simulations and experiments conducted with the RM instrument have shown that the reflectron is not perfectly compensating the differences in the initial kinetic energies of the secondary ions and that the slower ions are following a shorter path leading to a shorter TOF. Thus, the TOF is slightly decreased when the potential of the surface is increasing. Since the intensity of the primary ion beam is not spatially constant (approximately a Gaussian profile), there is a gradient in the electrical potential at the particle's surface and the same ion species will arrive at different TOF on the detector, leading to the apparition of this left-hand shoulder. Thus, the presence of this left-hand shoulder on some negative ion peaks is characteristic of ions produced from an electrostatically charged surface, i.e. the surface of the cometary particles (Hornung et al., in preparation). Such effects, arising during the analyses of insulating samples, have already been thoroughly studied by Lee et al. (2012).

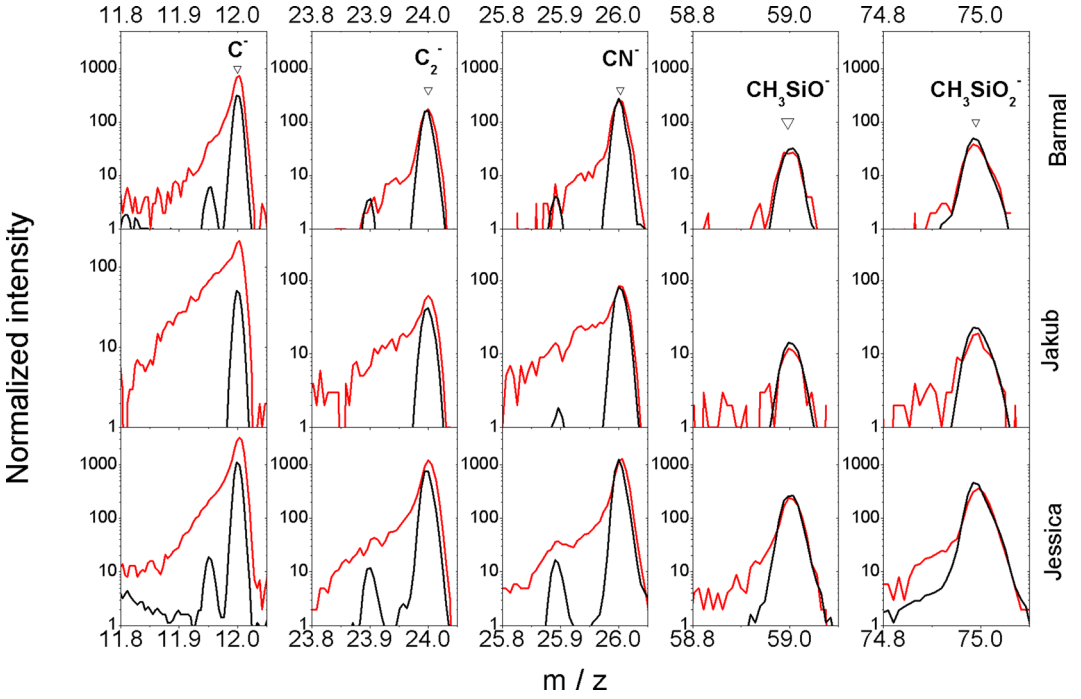

Figure 2. Typical negative ion TOF-SIMS spectra of cometary particles and targets of those particles. The spectra displayed in red are the sum of several individual spectra acquired on three cometary particles, Barmal (top), Jakub (middle) and Jessica (bottom). The spectra displayed in black were acquired on their respective gold targets, near the cometary particles of interest and at the same date as the spectra obtained on the particles. They have been normalized to the intensity of the PDMS fragments present in the mass spectra measured on the cometary particles. The three first columns show the C^-, C_2^- and CN^- peaks for which numerous ions are formed from the particles themselves, whereas the two last columns show two characteristic fragments of PDMS (CH_3SiO^- and $CH_3SiO_2^-$), which are entirely due to the surface contamination.

Moreover, we can note that this effect is not supposed to have an influence on the CN^-/C_2^- ionic ratio. In Fig. 2, it can be observed that for the three particles, the C^- peaks present a large left-hand shoulder, showing that numerous C^- ions originate from the surface of the particle. This left-hand shoulder is also clearly visible for the C_2^- and CN^- ions. Thus, it is possible to determine the fraction of the C_2^- and CN^- ions produced from the surface of the cometary particles.

In this study, we are considering the analyses performed on 27 cometary particles (see Table 2). They were all collected on gold collection target plates covered by a nano-porous gold layer (Hornung et al. 2014). Their equivalent diameters are ranging from 70 to nearly 400 μm (see Table 2). Thus, the size of some cometary particles is comparable to the size of the primary ion beam. Most of the time, the secondary ions are predominantly emitted from the particles themselves, though there is always a contribution from the surrounding target. Therefore, it is essential to remove this non-cometary contribution from the spectra. As for the calibration samples, for a given cometary particle, most of the time the analysis is carried out with a line scan or a matrix scan covering a large area on the particle and next to it. For each cometary particle included in this study (Table 2), we have selected negative ion mass spectra with the lowest intensities of gold and PDMS. These spectra are considered as being acquired on the particle. Moreover, some peaks, especially C^- and O^- ions, display the characteristic left-hand shoulder of secondary ions originating from the surface of the particles. Nevertheless, and especially for the smallest particles, a part of the secondary ions are also coming from the target's surface, resulting into a small fraction coming from the dust particles. We have also selected some spectra obtained at the same date and near the considered particles with a high intensity of gold and PDMS. This second set of spectra does not display a left-hand shoulder for the peaks, indicating that all the ions are originating from a surface at the nominal potential, i.e. the surface of the conductive collection target made of gold (see Fig. 2). In this second set of spectra, the cometary contribution is negligible. Careful examinations of all the spectra do not reveal a change of the surface contamination between the target and the particle positions. Thus, we have considered that the signature of the surface contamination is the same on the particles and on the target.

For all the spectra, C_2^-, CN^-, CH_3SiO^- and $CH_3SiO_2^-$ peaks were integrated over their whole width, including the left-hand shoulder. First, we calculate the intensity ratios of the two main ions of PDMS (CH_3SiO^- and $CH_3SiO_2^-$) between the mass spectra acquired on the particles and on the target. The value of these two ratios is always very similar and a normalization factor f is obtained by averaging both ratios. In the mass spectra measured on the particles, the contribution of the contamination needs to be subtracted in order to retrieve the number of C_2^- and CN^- ions that are really coming from the cometary particles. The number of CN^- ions in the spectra measured on the target is subtracted from the one obtained on the particles after normalization to the PDMS intensity using the previous normalization factor f using the following equation:

$$CN^- = CN^-_{\text{particles}} - (CN^-_{\text{target}} \times f). \quad (1)$$

The same methodology is used for C_2^-. Finally, the CN^-/C_2^- ion ratio is calculated (see Table 2). A similar procedure has already been used to handle the COSIMA positive mode data (Hilchenbach et al. 2016; Paquette et al. 2016; Bardyn et al. 2017; Stenzel et al. 2017).

Table 2. 67P particles considered for the measurements of their N/C atomic ratio, along with their collection target, collection period with starting date and total exposure time, their analysis date, typology, CN^-/C_2^- ion ratio and N/C atomic ratio. The typology refers to that presented in Langevin et al. (2016). C, S, G and R stand for Compact particles, Shattered clusters, Glued clusters and Rubble piles, respectively.

	Target	Particle name	Collection period	Starting date of the collection period	Total exposure time (days)	Analysis date	Area (px^2)	Area (um^2)	Eq. diameter (um)	Typology of the particles	CN^-/C_2^-	N/C (at.)
1	3D0	Kerttu	Rikkavesi	18/10/2014	6.62	26/03/2016	275	27 048	185.6	C	1.17 ± 0.03	0.047 ± 0.012
2	1CF	Atika	Ala-Kitka	16/12/2014	3.71	03/02/2016	95	18 620	154	G	0.80 ± 0.30	0.032 ± 0.024
3	2CF	Jean-Pierre	Kolima.3	24/01/2015	1.02	04/02/2016	432	84 672	328.4	S	0.94 ± 0.12	0.038 ± 0.018
4	2CF	Sami	Kolima.3	24/01/2015	1.02	08/01/2016	73	14 308	135	S	0.60 ± 0.09	0.024 ± 0.015
5	2CF	Jessica	Lummene.2	26/01/2015	0.97	04/02/2016	582	114 072	381.2	S	0.65 ± 0.01	0.026 ± 0.011
6	3C7	Spencer	Inari	22/02/2015	4.72	12/11/2015	21	4116	72.4	C	0.72 ± 0.13	0.029 ± 0.016
7	3C7	Juvenal	Kolima	02/03/2015	7.11	29/04/2015	35	6860	93.5	C	1.02 ± 0.04	0.041 ± 0.013
8	2D1	David	Toisvesi.2	11/05/2015	0.76	12/06/2015	155	30 380	196.7	S	1.20 ± 0.18	0.048 ± 0.018
9	2D1	Francesco	Toisvesi.2	11/05/2015	0.76	17/06/2015	382	74 872	308.8	R	1.00 ± 0.09	0.040 ± 0.015
10	2D1	Jakub	Toisvesi.2	11/05/2015	0.76	12/06/2015	430	84 280	327.7	S	1.23 ± 0.05	0.049 ± 0.013
11	2D1	Kenneth	Toisvesi.2	11/05/2015	0.76	17/06/2015	142	27 832	188.3	R	0.55 ± 0.26	0.022 ± 0.021
12	2D1	Roberto	Toisvesi.2	11/05/2015	0.76	17/06/2015	21	4116	72.4	S	1.05 ± 0.10	0.042 ± 0.015
13	1CD	Umeka	Jonkeri.2	03/07/2015	1.38	20/08/2015	38	7448	97.4	G	0.46 ± 0.05	0.018 ± 0.013
14	2CD	Amani	Nilakka.7	25/07/2015	1.19	06/08/2015	31	6076	88.0	G	1.30 ± 0.35	0.052 ± 0.025
15	2CD	Aril	Nilakka.7	25/07/2015	1.19	06/08/2015	39	7644	98.7	G	1.07 ± 0.36	0.043 ± 0.025
16	2CD	Karen	Nilakka.7	25/07/2015	1.19	30/09/2015	280	54 880	264.4	S	0.55 ± 0.02	0.022 ± 0.011
17	1CD	Barmal	Orivesi.4	31/07/2015	0.84	13/08/2015	83	16 268	144.0	R	1.50 ± 0.27	0.060 ± 0.022
18	1CD	Blat	Orivesi.4	31/07/2015	0.84	15/10/2015	130	25 480	180.2	R	0.90 ± 0.02	0.036 ± 0.012
19	1CD	Bonin	Orivesi.4	31/07/2015	0.84	20/08/2015	109	21 368	165	R	0.92 ± 0.13	0.037 ± 0.016
20	1CD	Bregan	Orivesi.4	31/07/2015	0.84	20/08/2015	66	12 936	128.4	G	0.96 ± 0.23	0.038 ± 0.020
21	1D2	Enton	Hankavesi.1	23/10/2015	6.46	19/11/2015	21	4116	72.4	G	0.45 ± 0.24	0.018 ± 0.020
22	1D2	Juliette	Hankavesi.1	23/10/2015	6.46	18/11/2015	76	14 896	137.8	G	0.70 ± 0.09	0.028 ± 0.01
23	1D2	Eris	Kolima.2	16/11/2015	1.61	25/11/2015	30	5880	86.5	G	0.58 ± 0.14	0.023 ± 0.017
24	1D2	Fadil	Kolima.2	16/11/2015	1.61	25/11/2015	45	8820	106.0	G	0.79 ± 0.27	0.032 ± 0.021
25	1D2	Sophie	Kolima.2	16/11/2015	1.61	25/11/2016	75	14 700	136.8	R	0.85 ± 0.04	0.034 ± 0.013
26	2D2	Stefane	Ukonvesi.6	17/01/2016	0.86	11/02/2016	35	6860	93.5	R	0.56 ± 0.05	0.022 ± 0.013
27	1D2	Günter	Jerisjarvi.1	29/02/2016	0.75	14/04/2016	540	105 840	367.2	R	1.26 ± 0.19	0.050 ± 0.019

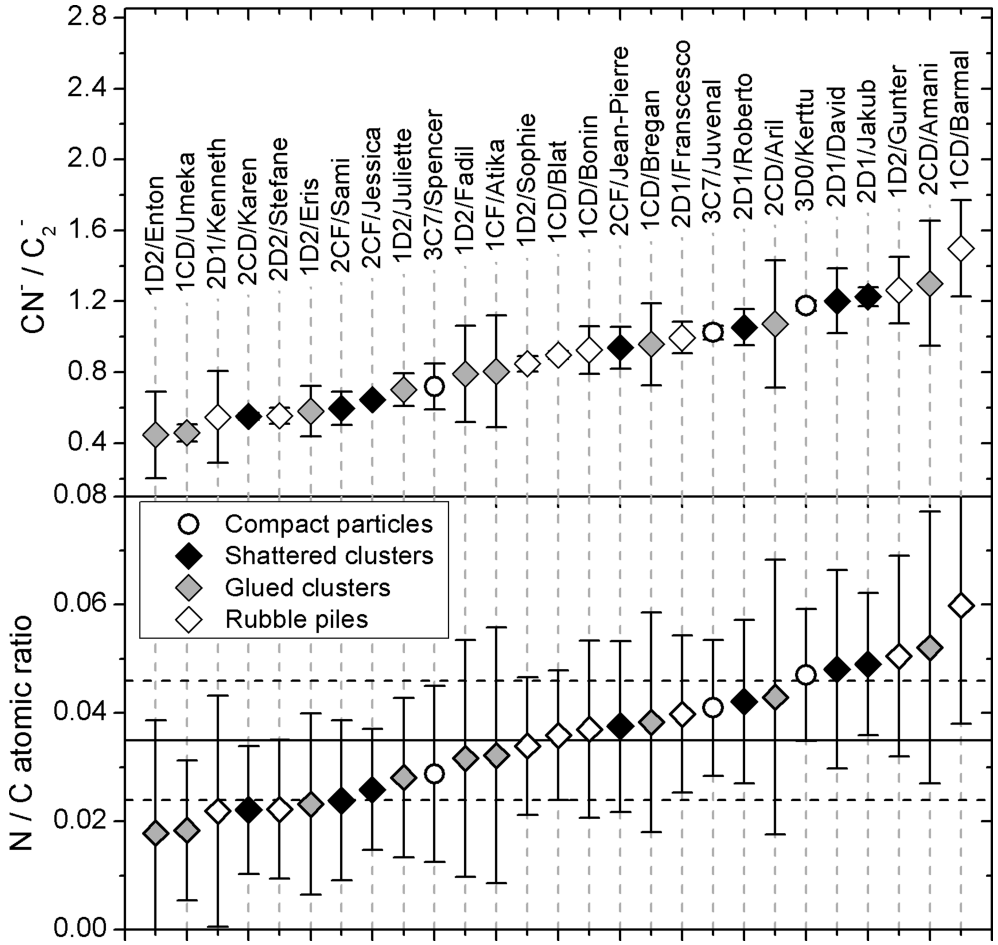

Figure 3. CN^-/C_2^- ion ratios (upper panel) and N/C atomic ratios (lower panel) of the 27 considered cometary particles arranged by increasing N/C atomic ratios. The different symbols stand for the different typologies of cometary particles as defined by Langevin et al. (2016). We have considered three compact particles, seven shattered clusters, nine glued clusters and eight rubbles piles. The horizontal lines in the lower panel represent the average of the N/C atomic ratio of 0.035 ± 0.011.

3 RESULTS AND DISCUSSION

The bulk CN^-/C_2^- ion ratios measured on the 27 particles of comet 67P yield N/C atomic ratios ranging from 0.018 to 0.060 (see Table 2 and Figs 3–5). Taking into account the predicted 68 per cent level of confidence in the calibration curve, the error bars of the N/C atomic ratios range between 25 and 100 per cent. By averaging the values of all the considered cometary particles, we find an averaged N/C atomic ratio of 0.035 ± 0.011. Fig. 3 presents the CN^-/C_2^- ion ratios as well as the N/C atomic ratios measured on the 27 considered cometary particles. The ion ratio seems to vary significantly from one particle to another. However, due to the dispersion of the measurements on the calibration samples, which leads to a large uncertainty in the calibration line, nearly all the N/C values are consistent with a value of 0.035. Despite the apparent variation of the CN^-/C_2^- ion ratios, the possibility remains that all the particles have roughly the same N/C atomic ratio.

It has already been shown that the cometary particles collected by the COSIMA instrument have different morphologies and they were classified into four typologies (Langevin et al. 2016). It is tempting to try to associate these different typologies with diverse compositions. Therefore, we have searched for a correlation between the CN^-/C_2^- ion ratio and the morphology of the considered particles. To date, no correlation between the composition and the typologies

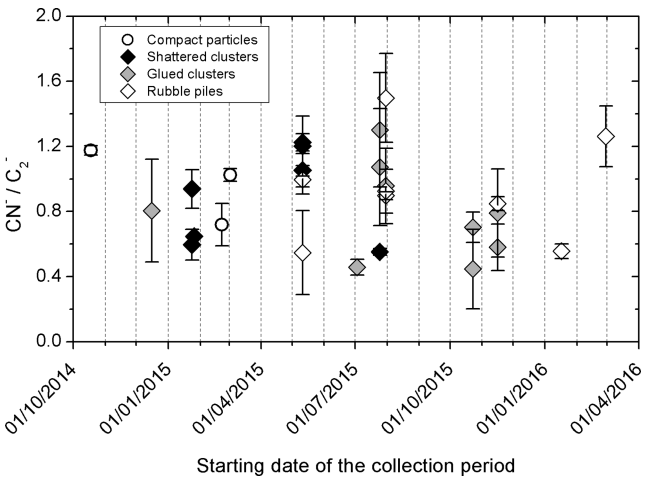

Figure 4. CN^-/C_2^- ion ratios of the 27 considered cometary particles as a function of their collection date. The different symbols stand for the different typologies of cometary particles as defined by Langevin et al. (2016).

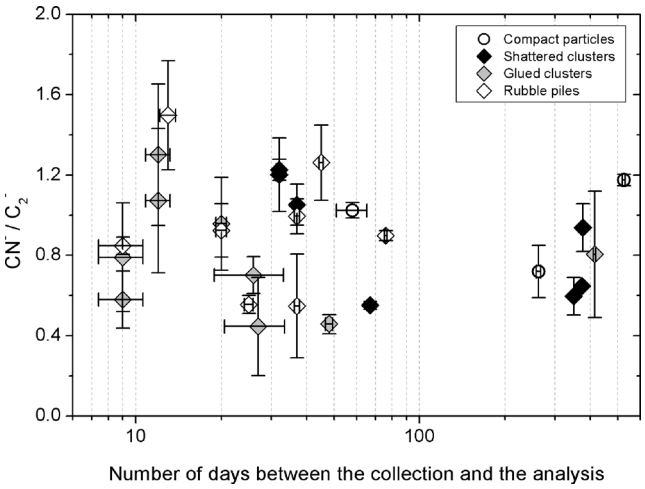

Figure 5. CN^-/C_2^- ion ratios of the 27 considered cometary particles as a function of the time interval between their collection and analysis. The different symbols stand for the different typologies of cometary particles as defined by Langevin et al. (2016).

of the cometary particles has been found (see Fig. 3). Fig. 4 presents the CN^-/C_2^- ion ratios as a function of the collection date of the particle. The objective was to search for an evolution of the composition of the cometary particles with the collection date or with the heliocentric distance at which the particles were collected. Such an evolution is not shown from our data (see Fig. 4). The cometary particles were stored in the COSIMA instrument at temperatures of about 283 K between their collection and analysis. If they still contained volatile organic compounds at the time of their collection, they could have sublimated during storage, changing the CN^-/C_2^- ion ratios with time. Thus, we also searched for a correlation between the CN^-/C_2^- ion ratios and the time intervals between the collection and the analysis of the particles (see Fig. 5). Again, no correlation was found, and no temporal evolution of the CN^-/C_2^- ion ratio of the cometary particles after their collection can be reported. As a conclusion, the CN^-/C_2^- ion ratios, as well as the N/C atomic ratios of the organic matter present in the particles of 67P, are not related to their morphology, collection dates or residence time before analysis.

The N/C atomic ratios measured in the particles of 67P can be compared to the values found in other comets and other astronomical objects. The first analysis performed by the PUMA-1 instrument led to an estimation of the N/C atomic ratio of about 0.04 in the particles of comet 1P/Halley (Kissel & Krueger 1987). Subsequent analyses of the observations performed by the PUMA-1 instrument resulted in an averaged value of 0.052 ± 0.028 for the N/C atomic ratio (Jessberger et al. 1988; Jessberger et al. 1991). The examination of the carbonaceous *Stardust* samples, brought to the Earth from 81P/Wild 2, revealed a wide variety of composition, chemical functionality and atomic ratios (Keller et al. 2006; Sandford et al. 2006; Cody et al. 2008). However, the reported low abundance of organic material could have been a consequence of its degradation during the collection (Brownlee 2014). N/C atomic ratios ranging from 0.07 to 0.24 were first reported from XANES spectra (Sandford et al. 2006; Cody et al. 2008); nevertheless, subsequent analyses revealed that the most N-rich organic matter with N/C $>$ 0.2 is the most likely contamination (De Gregorio et al. 2011). N/C atomic ratios ranging from 0.03 to 0.12 and 0.002 to 0.18, respectively, were derived by the XANES and SIMS analyses of what appears to

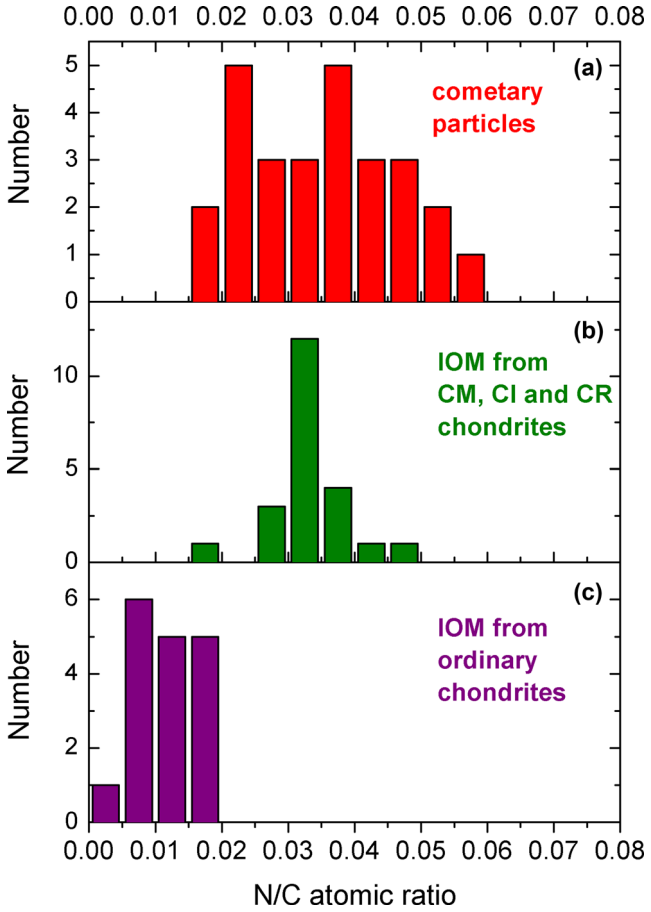

Figure 6. Histograms of the N/C atomic ratios measured in 27 cometary particles of 67P (in red, panel a), in 22 IOM samples of CI, CM and CR carbonaceous chondrites (in green, panel b) and in 17 IOM samples from ordinary chondrites (in purple, panel c). All the N/C atomic ratios of IOM samples of chondrites were found in Alexander et al. (2007).

be relatively unaltered, refractory cometary material (De Gregorio et al. 2011). The degree of variation in the N/C atomic ratio remains very large in the *Stardust* samples. The N/C atomic ratio measured in 67P particles (0.018 to 0.060) is in close agreement with the averaged value found in 1P/Halley and falls into the lower range of the values measured for the 81P/Wild 2 particles. The most striking difference is, however, the absence of any N/C ratio higher than 0.1 on the 67P particles.

Fig. 6 shows the distribution of the N/C atomic ratio measured in the cometary particles and in IOM samples extracted from unweathered chondrites (Alexander et al. 2007). As no value lower than 0.015 has been found in the 67P particles, the distribution of the N/C atomic ratio in these cometary particles is different from the one found in IOMs, when chondrites of all classes are considered (see Fig. 6). The lowest N/C values are only found in the IOMs extracted from ordinary chondrites that generally have a low carbon content. If we consider only the IOMs extracted from CM, CI and CR carbonaceous chondrites, the distribution of the N/C atomic ratios is similar to the one of 67P particles (see Fig. 6). This similitude between the N/C atomic ratios found in the IOMs from CM, CR, and CI chondrites and in the 67P particles confirms that the refractory organic matter contained in cometary particles shares some similarities with the IOMs of carbonaceous chondrites as already reported by Fray et al. (2016).

With values between 0.01 and 0.05, the bulk N/C atomic ratio in most IDPs and chondritic micrometeorites is compatible with that of carbonaceous chondrites (Matrajt et al. 2003). However, some sub-micrometer-sized units in IDPs present some N concentrations of 10–30 wt. per cent, which could indicate higher values of the N/C atomic ratio (Aleon et al. 2003; Floss et al. 2006). Generally, these hotspots are extremely ^{15}N-rich. However, Floss et al. (2010) report a large range of the N/C atomic ratios (0.03–0.5) for these ^{15}N-rich regions in one particular IDP of presumed cometary origin. These ^{15}N hotspots present in IDPs have been studied with a spatial resolution of $\sim$1.5 μm (Aleon et al. 2003) and of $\sim$100 nm (Floss et al. 2006). The XANES and nano-SIMS analyses performed on the *Stardust* samples have a spatial resolutions of 25 and 100 nm, respectively (De Gregorio et al. 2011), thus the N/C atomic ratio $>$0.1 found in the *Stardust* samples can tentatively be attributed to such specific hotspots. However, one has to keep in mind that the spatial resolution of COSIMA is about 35 $\times$ 50 μm^2, which makes the instrument not able to distinguish individual sub-micrometer units, such as the ones present in IDPs. The absence of an N/C atomic ratio $>$0.1 in the COSIMA measurements could be due to the spatial resolution of this instrument, which does not allow the detection of hotspots with sizes of the order of 1 μm. Thus, the measurements for the 67P particles have to be considered as bulk values. The range of N/C values measured in the 67P particles is compatible with the bulk values found in the IOMs samples extracted from carbonaceous chondrites as well as in bulk IDPs and micrometeorites (Matrajt et al. 2003; Alexander et al. 2007). Notable exceptions are the large bulk values (up to 0.20) of the N/C atomic ratio found in some UCAMMs, which are potentially of cometary origin (Duprat et al. 2010; Dartois et al. 2013). Nevertheless, it seems that N-poor and N-rich organic material can co-exist within this type of particles (Yabuta et al. 2012; Engrand et al. 2016; Charon et al. 2017). The N-rich organic material could have been formed by galactic cosmic ray irradiation of N_2- and CH_4-rich ices. Such a process could have occurred at the surface of a Kuiper belt or Oort cloud object beyond the nitrogen snow line (Dartois et al. 2013; Augé et al. 2016). As the large bulk N/C atomic ratio of the UCAMMs has not been found in the 67P particles, this process seems to be excluded for the synthesis of the organic matter found in 67P particles.

Bardyn et al. (2017) reported the average elemental abundances of C, O, Na, Mg, Al, Si, K, Ca, Cr, Mn and Fe in the cometary particles collected by the COSIMA instrument. Supposing that the H/C ratio is equal to 1 (Fray et al. 2016) and that S/Fe is chondritic, i.e. equal to 0.5 (see Lodders 2010), we can estimate that the carbon and nitrogen weights in 67P particles are about 31 $\pm$ 7 and 1.2 $\pm$ 0.6 wt. per cent, respectively. In carbonaceous chondrites, the highest carbon and nitrogen abundances are found in CI chondrites with values of about 3.5 and 0.2 wt. per cent (Kerridge 1985; Alexander et al. 2012). In some IDPs, the carbon abundance can be higher than in the most C-rich chondrites with values of about 12.5 wt. per cent (Thomas et al. 1993). The only extraterrestrial samples richer in carbon and in nitrogen than the 1P/Halley and 67P cometary particles are the UCAMMs, which present an exceptionally high carbon content (Duprat et al. 2010; Dartois et al. 2013). Therefore, with the exception of UCAMMs, the cometary particles analysed in the environment of comet 1P/Halley and comet 67P are the most C- and N-rich astronomical objects found so far. This indicates that cometary particles might have better preserved their original organic content and are much less altered than the objects with lower C and N abundances such as the carbonaceous chondrites. Furthermore, it indicates that comets have been aggregated in an organic-rich region of the protoplanetary disc. Nevertheless, the similar N/C atomic values of 1P/Halley, 67P and CM, CI and CR chondrites point towards a similar refractory organic matter in all these objects.

The analysis performed in the environment of comet 1P/Halley in 1986 showed that the C/Si atomic ratio of the particles and of the nucleus of 1P/Halley is close to the Solar value (Jessberger et al. 1988; Geiss 1987). However, the N/C and N/Si atomic ratios are about six times lower in 1P/Halley than in the Sun, showing that nitrogen is depleted in 1P/Halley compared to the Sun (Geiss 1987; Wyckoff et al. 1991). As for 1P/Halley, the carbon abundance in the 67P particles is close to the solar value (Bardyn et al. 2017). Nevertheless, as the N/C atomic ratio of the solar photosphere is about 0.3 $\pm$ 0.1 (Lodders 2010), it is clear that the particles collected in the environment of 67P, which have an averaged N/C atomic ratio of about 0.035, are depleted in nitrogen compared to the Sun. Thanks to the measurements performed by the ROSINA instrument aboard *Rosetta* at about 3.1 au from the Sun in 2014 October, we can estimate that the N/C atomic ratio of the gas phase is about 0.007 and 0.025 in the winter and summer hemispheres, respectively (Le Roy et al. 2015a). The subsequent detection of molecular nitrogen at an extremely low abundance does not significantly change the N/C ratio of the gas phase (Rubin et al. 2015). Moreover, an N/C atomic ratio lower than 0.25 seems to be typical for all the comets observed at infrared wavelengths (Dello Russo et al. 2016). Thus, the gas phase cannot account for the nitrogen depletion of the refractory organic matter present in the 67P particles. In conclusion, like 1P/Halley, the nucleus of 67P seems to be strongly depleted in nitrogen compared to the Sun.

4 CONCLUSIONS

The COSIMA mass spectrometer has performed *in situ* analyses of dust particles collected in the near environment of comet 67P. The measurement of the CN^-/C_2^- ion ratios enables the evaluation of the N/C atomic ratio in 27 individual dust particles. This atomic ratio ranges from 0.018 to 0.06 depending on the considered particle with an averaged value of 0.035 $\pm$ 0.011. The variations of the N/C ratio are not related to the morphology, collection date or residence time before analysis of the particles. The average values found in the 67P particles are consistent with most of the values found in the IOMs extracted from CM, CR and CI carbonaceous chondrites, and also with bulk IDPs and with the average values found in the dust of comet 1P/Halley (Jessberger et al. 1988; Matrajt et al. 2003; Alexander et al. 2007). As most of the carbon and nitrogen should reside in the refractory organic matter, the similarity of the N/C atomic ratio measured in cometary particles and in the most primitive carbonaceous chondrites strengthens the similitudes between the organic matters contained in these objects, even if the H/C atomic ratio could be slightly higher in the cometary organic matter (Fray et al. 2016). Based on these observations, a similar chemical origin of the cometary and meteoritic organic matter has to be considered as a viable hypothesis. Nevertheless, some hotspots found in IDPs as well as in some small organic units of the *Stardust* grains present an N/C atomic ratios higher than 0.1 (Aleon et al. 2003; De Gregorio et al. 2011). Such high values have also been found in bulk UCAMMs (Dartois et al. 2013), but not in the 67P particles. Although this could be due to the low spatial resolution of the COSIMA instrument, the absence of values higher than 0.1 for the N/C atomic ratio in the 67P particles could also point towards a different origin of the N-rich organic material in UCAMMs and the refractory organic material in the 67P particles. The N-rich carbonaceous matter of the UCAMMs could be formed in a N_2-rich

environment by irradiation processes (Dartois et al. 2013; Augé et al. 2016), but as the icy fraction of 67P is depleted in N_2 (Rubin et al. 2015), the 67P nucleus should not be a suitable environment to form organic matter with an N/C atomic ratio higher than 0.1.

Taking into account the elemental abundances measured by Bardyn et al. (2017) in the particles of 67P, and making an educated guesses for the H and S elemental abundances, we can estimate that the carbon and nitrogen weights of cometary particles are about 31 ± 7 wt. per cent and 1.2 ± 0.6 wt. per cent, respectively. Even if the N/C atomic ratio found in the 67P particles is similar to the one measured in bulk carbonaceous chondrites and IDPs, the global abundance of carbon (31 ± 7 wt. per cent) and nitrogen (1.2 wt. per cent) is quite high compared with the values found in carbonaceous chondrites and IDPs. Thus, the 67P particles and the nucleus are rich in organic matter, as already suggested from indirect observations (Fulle et al. 2016; Herique et al. 2016), and this indicates that comets have been aggregated in an organic-rich region of the protoplanetary disc.

Nevertheless, the cometary particles as well as the whole nucleus of comet 67P is strongly depleted in nitrogen compared to the Sun. A similar result has already been found for 1P/Halley (Geiss 1987; Wyckoff et al. 1991). Therefore, this nitrogen depletion could constrain the formation scenarios of cometary nuclei.

It has already been shown that the H/C and N/C atomic ratios are fairly well correlated in the IOMs of carbonaceous chondrites (Alexander et al. 2007). Although the measurements of the H abundance will be extremely challenging, future works with the COSIMA data will attempt to find any such correlation as well as an estimate of the $^{15}N/^{14}N$ isotopic ratio to state more precisely the possible formation place of the cometary refractory organic matter.

ACKNOWLEDGEMENTS

COSIMA was built by a consortium led by the Max-Planck-Institut für Extraterrestrische Physik, Garching, Germany in collaboration with Laboratoire de Physique et Chimie de l'Environnement et de l'Espace, Orléans, France, Institut d'Astrophysique Spatiale, CNRS/Université Paris Sud, Orsay, France, Finnish Meteorological Institute, Helsinki, Finland, Universität Wuppertal, Wuppertal, Germany, von Hoerner und Sulger GmbH, Schwetzingen, Germany, Universität der Bundeswehr, Neubiberg, Germany, Institut für Physik, Forschungszentrum Seibersdorf, Seibersdorf, Austria, Institut für Weltraumforschung, Österreichische Akademie der Wissenschaften, Graz, Austria and is led by the Max-Planck-Institut für Sonnensystemforschung, Göttingen, Germany. We thank F. Brandstätter, L. Ferrière and C. Koeberl from the Natural History Museum Vienna for providing bulk meteorite samples as well as H. Krüger for technical assistance in the COSIMA RM operations and sample handling. The support of the national funding agencies of Germany (DLR, grant 50 QP 1302), France (CNES), Austria (Austrian Science Fund, FWF, project P 26871-N20), Finland and the ESA Technical Directorate is gratefully acknowledged. AB acknowledges support from the CNES and the Labex Exploration Spatiale des Environnements Planétaires (ESEP; no. 2011-LABX-030) and funding from the Idex Paris Sciences et Lettres (PSL; no. ANR-10-IDEX-0001-02). RI also acknowledges support from the Labex Exploration Spatiale des Environnements Planétaires (ESEP; no. 2011-LABX-030) and funding from the Idex Paris Sciences et Lettres (PSL; no. ANR-10-IDEX-0001-02). SS acknowledges funding from the Swedish National Space Board (contracts 121/11 and 198/15). We thank the Rosetta Science Ground Segment at ESAC, the *Rosetta* Mission Operations Centre at ESOC and the Rosetta Project at ESTEC for their outstanding work enabling the science return of the *Rosetta* Mission. *Rosetta* is an ESA mission with contributions from its Member States and NASA.

REFERENCES

Aleon J., Robert F., Chaussidon M., Marty B., 2003, Geochim. Cosmochim. Acta, 67, 3773
Alexander C. M. O. D., Bowden R., Fogel M. L., Howard K. T., Herd C. D. K., Nittler L. R., 2012, Science, 337, 721
Alexander C. M. O. D., Fogel M., Yabuta H., Cody G. D., 2007, Geochim. Cosmochim. Acta, 71, 4380
Augé B. et al., 2016, A&A, 592, A99
Bardyn A. et al., 2017, MNRAS, in press
Bentley M. S. et al., 2016, Nature, 537, 73
Brownlee D., 2014, Ann. Rev. Earth Planet Sci., 42, 179
Brownlee D. et al., 2006, Science, 314, 1711
Brownlee D. E., 2016, Elements, 12, 165
Charon E. et al., 2017, Lunar Planet Sci., 48, 1964
Clark B. C., Mason L. W., Kissel J., 1987, A&A, 187, 779
Cody G. D. et al., 2008, Meteorit. Planet. Sci., 43, 353
Dartois E. et al., 2013, Icarus, 224, 243
De Gregorio B. T., Stroud R. M., Cody G. D., Nittler L. R., Kilcoyne A. L. D., Wirick S., 2011, Meteorit. Planet. Sci., 46, 1376
Della Corte V. et al., 2015, A&A, 583, A13
Dello Russo N., Kawakita H., Vervack R. J., Jr, Weaver H. A., 2016, Icarus, 278, 301
Dobrica E., Engrand C., Duprat J., Gounelle M., Leroux H., Quirico E., Rouzaud J. N., 2009, Meteorit. Planet. Sci., 44, 1643
Duprat J. et al., 2010, Science, 328, 742
Elsila J. E., Glavin D. P., Dworkin J. P., 2009, Meteorit. Planet. Sci., 44, 1323
Engrand C. et al., 2016, MNRAS, 462, S323
Floss C., Stadermann F. J., Bradley J. P., Dai Z. R., Bajt S., Graham G., Lea A. S., 2006, Geochim. Cosmochim. Acta, 70, 2371
Floss C., Stadermann F. J., Mertz A. F., Bernatowicz T. J., 2010, Meteorit. Planet. Sci., 45, 1889
Flynn G. J., Nittler L. R., Engrand C., 2016, Elements, 12, 177
Fomenkova M. N., 1999, Space Sci. Rev., 90, 109
Fomenkova M. N., Chang S., Mukhin L. M., 1994, Geochim. Cosmochim. Acta, 58, 4503
Fray N. et al., 2016, Nature, 538, 72
Fulle M. et al., 2016, MNRAS, 462, S132
Geiss J., 1987, A&A, 187, 859
Glassmeier K. H., Boehnhardt H., Koschny D., Kuhrt E., Richter I., 2007, Space Sci. Rev., 128, 1
Henkel T., Gilmour J., 2014, in Turekian K. K., ed., Treatise on Geochemistry, 2nd edn. Elsevier, Oxford, p. 411
Herique A. et al., 2016, MNRAS, 462, S516
Hilchenbach M. et al., 2017, Phil. Trans. R. Soc. A, 375, 20160255
Hilchenbach M. et al., 2016, ApJ, 816, L32
Hornung K. et al., 2014, Planet.Space Sci., 103, 309
Hornung K. et al., 2016, Planet.Space Sci., 133, 63
Jessberger E. K., Christoforidis A., Kissel J., 1988, Nature, 332, 691
Jessberger E. K., Kissel J., Neugebauer M., Rahe J., 1991, in Newburn R. L., Jr, ed., Proc. IAU Colloq. 116, Comets in the Post-Halley Era. Kluwer, Dordrecht, p. 1075
Keller L. P. et al., 2006, Science, 314, 1728
Keller L. P., Messenger S., Flynn G. J., Clemett S., Wirick S., Jacobsen C., 2004, Geochim. Cosmochim. Acta, 68, 2577
Kerridge J. F., 1985, Geochim. Cosmochim. Acta, 49, 1707
Kissel J. et al., 2007, Space Sci. Rev., 128, 823
Kissel J. et al., 1986a, Nature, 321, 336
Kissel J., Krueger F. R., 1987, Nature, 326, 755
Kissel J., Krueger F. R., Silen J., Clark B. C., 2004, Science, 304, 1774
Kissel J. et al., 1986b, Nature, 321, 280
Krueger H. et al., 2015, Planet. Space Sci., 117, 35

Langevin Y. et al., 2016, Icarus, 271, 76
Langevin Y., Kissel J., Bertaux J. L., Chassefiere E., 1987, A&A, 187, 761
Lawler M. E., Brownlee D. E., 1992, Nature, 359, 810
Lee J. L. S., Qiao Y., Cheng X., Yan Y., Li Z., Huang J., 2012, Surf. Interface Anal., 44, 238
Le Roy L. et al., 2015a, A&A, 583, A1
Le Roy L., Bardyn A., Briois C., Cottin H., Fray N., Thirkell L., Hilchenbach M., 2015b, Planet. Space Sci., 105, 1
Le Roy L., Briani G., Briois C., Cottin H., Fray N., Thirkell L., Poulet G., Hilchenbach M., 2012, Planet. Space Sci., 65, 83
Lodders K., 2010, in Goswami A., Reddy B. E., eds., Astrophysics and Space Science Proc., Principles and Perspectives in Cosmochemistry. Springer-Verlag, Berlin, p. 379
Matrajt G., Taylor S., Flynn G., Brownlee D., Joswiak D., 2003, Meteorit.Planet. Sci., 38, 1585
Merouane S. et al., 2016, A&A, 596, A87
Merouane S. et al., 2017, MNRAS, in press
Paquette J. A., Engrand C., Stenzel O., Hilchenbach M., Kissel J., the COSIMA Team, 2016, Meteorit. Planet. Sci., 51, 1340
Reinhard R., 1986, Nature, 321, 313
Rotundi A. et al., 2015, Science, 347, aaa3905
Rubin M. et al., 2015, Science, 348, 232
Sagdeev R. Z., Blamont J., Galeev A. A., Moroz V. I., Shapiro V. D., Shevchenko V. I., Szego K., 1986, Nature, 321, 259
Sandford S. A. et al., 2006, Science, 314, 1720
Sandford S. A. et al., 2010, Meteorit. Planet. Sci., 45, 406
Sandford S. A., Engrand C., Rotundi A., 2016, Elements, 12, 185
Stenzel O. et al., 2017, MNRAS, in press
Thomas K. L., Blanford G. E., Keller L. P., Klock W., McKay D. S., 1993, Geochim. Cosmochim. Acta, 57, 1551
Thomen A., Robert F., Remusat L., 2014, J. Anal. Atom. Spectrom., 29, 512
Vickerman J. C., Briggs D., 2013, in Vickermann J. C., Briggs D. eds, TOF-SIMS: Materials analysis by mass spectrometry. IMP Publ., Chichester, p. 1
Willacy K. et al., 2015, Space Sci. Rev., 197, 151
Wyckoff S., Tegler S. C., Engel L., 1991, ApJ, 367, 641
Yabuta H. et al., 2012, Lunar Planet. Sci., 43, 2239

[1]*Laboratoire Interuniversitaire des Systèmes Atmosphériques (LISA), UMR CNRS 7583, Institut Pierre Simon Laplace, Université Paris Est Créteil et Université Paris Diderot, F-94000 Créteil, France*
[2]*Laboratoire de Physique et Chimie de l'Environnement et de l'Espace (LPC2E), UMR CNRS 7328, Université d'Orléans, F-45071 Orléans, France*
[3]*Institut d'Astrophysique Spatiale (IAS), CNRS/Université Paris Sud, Bâtiment 121, F-91405 Orsay, France*
[4]*Centre de Sciences Nucléaires et de Sciences de la Matière (CSNSM), CNRS/IN2P3 – Univ. Paris Sud – UMR 8609, Université Paris-Saclay, Bâtiment 104, F-91405 Orsay campus, France*
[5]*Max-Planck-Institut für Sonnensystemforschung (MPS), Justus-von-Liebig-Weg 3, D-37077 Göttingen, Germany*
[6]*Universität der Bundeswehr LRT-7, Werner Heisenberg Weg 39, D-85577 Neubiberg, Germany*
[7]*Tuorla Observatory, Department of Physics and Astronomy, University of Turku, Väisäläntie 20, FI-21500 Piikkiö, Finland*
[8]*Center for Space and Habitability (CSH), University of Bern, Sidlerstrasse 5, CH-3012 Bern, Switzerland*
[9]*Institut de Planétologie et d'Astrophysique de Grenoble (IPAG), UMR 5274, Univ. Grenoble Alpes, CNRS, F-38000 Grenoble, France*
[10]*Finnish Meteorological Institute, Observation services, Erik Palménin aukio 1, FI-00560 Helsinki, Finland*
[11]*European Space Agency (ESA), Scientific Support Office, Keplerlaan 1, Postbus 299, NL-2200 AG Noordwijk, the Netherlands*
[12]*RISE Research Institutes of Sweden, Bioscience and Materials, Chemistry, Materials and Surfaces, Box 5607, SE-114 86 Stockholm, Sweden*
[13]*Institute of Statistics and Mathematical Methods in Economics, Vienna University of Technology, Wiedner Hauptstrasse 7/105-6, A-1040 Vienna, Austria*

This paper has been typeset from a Microsoft Word file prepared by the author.